

Ioneutral control of effective diapycnal mixing in numerical ocean models with neutral rotated diffusion tensors

Antoine Hochet¹, Rémi Tailleux¹, David Ferreira¹, and Till Kuhlbrodt^{1,2}

¹Department of Meteorology, University of Reading

²National Center for Atmospheric Science

Correspondence to: a.hochet@reading.ac.uk

Abstract. A key challenge in numerical ocean modeling is the parameterisation of the turbulent mixing of heat and salt. Current models mostly use a rotated diffusion tensor based on mixing directions parallel and perpendicular to the local neutral vector. However, there is no density variable that is exactly neutral everywhere because of the coupling between thermobaricity and density-compensated temperature and salinity anomalies. Hence, when using neutral rotated diffusion, the effective diapycnal diffusivity experienced by any possible density variable is necessarily partly controlled by isoneutral diffusion. Here, this effect is quantified by evaluating the effective diapycnal diffusion coefficient for five widely used density variables: Jackett and McDougall (1997) γ^n , Lorenz reference state density ρ_{ref} of Saenz et al. (2015), and three potential density variables σ_0 , σ_2 and σ_4 . Computations are based on the World Ocean Circulation Experiment climatology, assuming either a uniform value for the isoneutral mixing coefficient or spatially varying values inferred from an inverse calculation. Isopycnal mixing contributions to the effective diapycnal mixing yield values consistently larger than 10^{-3} m²/s in the deep ocean for all density variables, with γ^n suffering the least from the isoneutral control of effective diapycnal mixing, and σ_0 the most. These high values are due to spatially localised large values of non-neutrality, mostly in the deep Southern Ocean. Removing only 5% of these high values on each density surface reduces the effective diapycnal diffusivities to less than 10^{-4} m²/s. This work highlights the conceptual and practical difficulties of relating the diapycnal mixing diffusivities inferred from global budgets or inverse methods relying on Walin-like water mass analyses to locally defined dianeutral diffusivities. Doing so requires being able to tease out the relative contribution of isoneutral mixing from the effective diapycnal mixing, and makes it difficult to study diapycnal mixing completely independently of isopycnal mixing. Because Lorenz reference density is not exactly neutral, isoneutral mixing contamination also pertains to the determination of spurious diapycnal mixing based on monitoring the evolution of Lorenz reference state, which has been overlooked so far.

20 1 Introduction

Simulations of climate change by means of coupled ocean-atmosphere numerical models are sensitive to parameterisations of oceanic sub-grid scale mixing of heat and salt. Indeed, sub-grid scale mixing processes directly control ocean heat uptake, the strength of the Atlantic meridional overturning circulation, and the poleward heat transport e.g., Kuhlbrodt and Gregory (2012). Because tracers are stirred and mixed preferentially along isopycnal surfaces, it has become commonly accepted following

Redi (1982) to mix potential temperature (alternatively Conservative Temperature) and salinity by means of a rotated diffusion tensor, namely:

$$\mathbf{K} = K_i(\mathbf{I} - \mathbf{d}\mathbf{d}^T) + K_d\mathbf{d}\mathbf{d}^T. \quad (1)$$

In (1), \mathbf{d} denotes a unit vector normal to the isopycnal surface considered (the diapycnal direction), K_i and K_d are the isopycnal and diapycnal mixing coefficients respectively, \mathbf{I} denotes the identity matrix, and the subscript T denotes transposition. Rotated diffusion decomposes the diffusive part of the turbulent fluxes of heat and salt $\mathbf{F}_\theta = \langle \mathbf{v}'\theta' \rangle_{\text{diffusive}} = -[K_i\nabla_i\theta + K_d\nabla_d\theta]$ and $\mathbf{F}_S = \langle \mathbf{v}'S' \rangle_{\text{diffusive}} = -[K_i\nabla_iS + K_d\nabla_dS]$ into orthogonal isopycnal and diapycnal components. These are $\nabla_i C = \nabla C - \mathbf{d}(\mathbf{d}^T\nabla C) = \nabla C - (\nabla C \cdot \mathbf{d})\mathbf{d}$ and $\nabla_d C = \mathbf{d}(\mathbf{d}^T\nabla C) = (\nabla C \cdot \mathbf{d})\mathbf{d}$ respectively, for $C = (S, \theta)$ and for some Reynolds averaging operator $\langle \cdot \rangle$. Here, θ is the potential temperature and S the salinity of standard seawater¹. This approach implies that K_i and K_d are linked to \mathbf{F}_θ and \mathbf{F}_S as follows:

$$K_i = -\frac{\mathbf{F}_\theta \cdot \nabla_i \theta}{|\nabla_i \theta|^2} = -\frac{\mathbf{F}_S \cdot \nabla_i S}{|\nabla_i S|^2}, \quad K_d = -\frac{\mathbf{F}_\theta \cdot \nabla_d \theta}{|\nabla_d \theta|^2} = -\frac{\mathbf{F}_S \cdot \nabla_d S}{|\nabla_d S|^2}. \quad (2)$$

As is well known, there is an infinite number of possible ways to define a density variable in a salty ocean with a realistic nonlinear equation of state. For instance, potential density $\sigma = \rho(S, \theta, p_r)$ defined relative to one particular reference pressure p_r is always different from potential density defined relative to a different reference pressure. A priori, each possible density variable can serve as the basis for a rotated diffusion tensor. However, the relations (2) show that K_i and K_d must then depend on the choice of the density variable. For lack of theoretical understanding on how to define isopycnal surfaces from first principles in the ocean, the diapycnal direction \mathbf{d} in (1) is currently specified in terms of the so-called neutral vector $\mathbf{N} = g(\alpha\nabla\theta - \beta\nabla S)$ as $\mathbf{d} = \mathbf{N}/|\mathbf{N}|$, e.g., McDougall et al. (2014), where α and β are the thermal expansion and haline contraction respectively, g being the acceleration of gravity. As shown by McDougall (1987a)'s work, the neutral directions (i.e. perpendicular to the neutral vector \mathbf{N}) hold special importance in the ocean as the directions along which two fluid parcels can swap position without experiencing buoyancy forces.

The adoption of rotated diffusion tensors (1) is relatively recent, however. Historically, early numerical ocean models had used a diffusion tensor based on mixing heat and salt with different mixing diffusivities in the horizontal and vertical directions. Following Veronis (1975), it has been generally assumed that such an approach causes spurious upwelling in western boundary currents owing to the unphysical diapycnal mixing component due to the large horizontal mixing across sloping isopycnal surfaces, the so-called "Veronis effect". The diffusive flux of any mathematically well-defined material density variable $\gamma(S, \theta)$, for such a mixing tensor is given by:

$$\mathbf{F}_\gamma = -K_H[\nabla\gamma - (\nabla\gamma \cdot \mathbf{k})\mathbf{k}] - K_V(\nabla\gamma \cdot \mathbf{k})\mathbf{k}, \quad (3)$$

where K_H and K_V are the horizontal and vertical mixing coefficients respectively, and \mathbf{k} the unit normal vector pointing upwards. Therefore, the diapycnal flux of \mathbf{F}_γ through an isopycnal surface $\gamma(S, \theta) = \text{constant}$ is given by:

$$\mathbf{F}_\gamma \cdot \frac{\nabla\gamma}{|\nabla\gamma|} = -[K_H \sin^2(\nabla\gamma, \mathbf{k}) + K_V \cos^2(\nabla\gamma, \mathbf{k})]|\nabla\gamma| = -[(K_H - K_V)\sin^2(\nabla\gamma, \mathbf{k}) + K_V]|\nabla\gamma|, \quad (4)$$

¹We assume fixed composition, thus allowing one to treat practical (conductivity) salinity and Absolute Salinity as equivalent, since the two are then linked to each other by a fixed conversion factor)

where $(\nabla\gamma, \mathbf{k})$ is the angle between the local gradient of γ and the vertical direction. This expression shows that the actual diapycnal mixing experienced by the density-like variable $\gamma(S, \theta)$ can be written as the sum $K_V + K_V^{Veronis}$, with:

$$K_V^{Veronis} = (K_H - K_V) \sin^2(\nabla\gamma, \mathbf{k}) \approx K_H \sin^2(\nabla\gamma, \mathbf{k}), \quad (5)$$

when $K_H \gg K_V$ as often assumed in ocean models. To the extent that it is legitimate to regard K_V as related to measured values of diapycnal/vertical mixing, it is generally assumed that $K_V^{Veronis}$ induces spurious diapycnal mixing whenever it exceeds K_V , which in general occurs whenever isopycnal slopes exceed some threshold depending on the relative ratio of K_d versus K_i . Rotated diffusion tensors, e.g., Redi (1982); McDougall and Church (1986), were introduced as a more natural and physical way to account for the 7 orders of magnitude difference between isopycnal and diapycnal mixing, and hence as a way to avoid the occurrence of the Veronis effect.

10 For tracer fields acted upon by rotated diffusion, the diffusive flux of any given material density variable $\gamma(S, \theta)$ is $\mathbf{F}_\gamma = \gamma_\theta \mathbf{F}_\theta + \gamma_S \mathbf{F}_S$, hence:

$$\mathbf{F}_\gamma = -K_i [\nabla\gamma - (\nabla\gamma \cdot \mathbf{d})\mathbf{d}] - K_d (\nabla\gamma \cdot \mathbf{d})\mathbf{d}, \quad (6)$$

where $\mathbf{d} = \mathbf{N}/|\mathbf{N}|$ is the normalized neutral vector, K_i and K_d the isoneutral and dianeutral turbulent mixing coefficient i.e. respectively perpendicular and parallel to the neutral vector. A conceptual difficulty with neutral rotated diffusion tensors,

15 however, is that it is not possible to construct for the ocean a mathematically well defined materially conserved variable $\gamma(S, \theta)$ allowing to write $\mathbf{N} = C_0 \nabla\gamma$, with C_0 some integrating factor. In the spatial domain, this can be attributed mathematically to the non-zero helicity of \mathbf{N} (see McDougall and Jackett (1988)). More instructive and illuminating, however, is to prove the result directly in thermohaline space. To that end, let us assume that such a variable γ exists, and show that it leads to a contradiction. To proceed, let us express in-situ density $\rho = \rho(S, \theta, p) = \hat{\rho}(\gamma, \theta, p)$ as a function of γ , θ and p for instance following Tailleux (2016b). The expression for the neutral vector becomes:

$$\mathbf{N} = -\frac{g}{\rho} \left(\frac{\partial \hat{\rho}}{\partial \gamma} \nabla\gamma + \frac{\partial \hat{\rho}}{\partial \theta} \nabla\theta \right) \quad (7)$$

where:

$$\frac{\partial \hat{\rho}}{\partial \theta} = \frac{1}{J} \frac{\partial(\gamma, \rho)}{\partial(S, \theta)} \quad (8)$$

where $J = \partial(\gamma, \theta)/\partial(S, \theta) = \partial\gamma/\partial S$ is the Jacobian of the transformation going from (S, θ) to (γ, θ) space. For γ to be exactly neutral would require $\partial\hat{\rho}/\partial\theta = 0$ everywhere, but Eq. (8) shows that this is impossible. Indeed, for $\partial(\gamma, \rho)/\partial(S, \theta)$ to be zero would require ρ to be a function of $\gamma(S, \theta)$ alone, but this cannot be true, because ρ also depends on pressure. This implies that the "effective diffusive mixing" experienced by a material density variable $\gamma(S, \theta)$, that is, the local diffusive flux of \mathbf{F}_γ through an iso- γ surface $\gamma = \text{constant}$ (or its surface-integrated value) must at least be partly controlled by isoneutral mixing, in a way that depends on the degree of non-neutrality of the density variable considered. Mathematically, the problem arises because the local concept of neutral mixing cannot be extended globally.

This idea is not entirely new, as it is closely connected to the concept of fictitious mixing discussed by McDougall and Jackett (2005) or Klocker et al. (2009) for instance. Physically, however, the concepts of effective diffusive mixing considered in the present paper and that of fictitious mixing have different purposes and implications. As alluded to above, the effective diffusivity of any particular density variable $\gamma(S, \theta)$ is simply the diffusivity K_d^γ 'seen' by such a variable when acted upon by a neutral rotated diffusion tensor. As clarified below, it is easily shown that $K_d^\gamma = K_i \sin^2(\mathbf{d}, \mathbf{N}) + K_d \cos^2(\mathbf{d}, \mathbf{N}) = K_d + (K_i - K_d) \sin^2(\mathbf{d}, \mathbf{N})$, where (\mathbf{d}, \mathbf{N}) is the angle made between $\mathbf{d} = \nabla\gamma/|\nabla\gamma|$ and \mathbf{N} . In contrast, the concept of fictitious mixing represents the extra diapycnal mixing $K_d^{fictitious} = (K_i - K_d) \sin^2(\mathbf{d}, \mathbf{N})$ through the local neutral tangent plane that would result from using a γ -based rotated diffusion tensor using the same mixing coefficients K_d and K_i . McDougall and Jackett (2005) or Klocker et al. (2009) use the term 'fictitious' because they assume that observations of diapycnal mixing inferred from tracer release experiments or microstructure measurements relate to diapycnal dispersion rather than dispersion through some other unspecified density surfaces. Assuming that direct observations of mixing relate to the diapycnal diffusivity K_d , the above considerations suggest that this is a priori not the case of the diapycnal diffusivity inferred from global budgets or inverse methods rooted in Walin (1982) type of water mass analysis. Indeed, such approaches usually rely on the use of a well defined thermodynamic material density variable such as σ_2 for instance, and must therefore a priori relate to the effective diapycnal diffusivity experienced by such a variable. Similarly, modern approaches to estimating spurious diapycnal mixing (Griffies et al., 2000; Ilıcak et al., 2012) rely on monitoring the evolution of Lorenz reference state entering the theory of available potential energy (Winters et al., 1995; Saenz et al., 2015) and are therefore related to the effective diapycnal diffusivity experienced by Lorenz reference density, not to the diapycnal diffusivity. As shown by Tailleux (2016a), Lorenz reference density can be written as $\rho_{ref} = \rho(S, \theta, p_r(S, \theta))$, where $p_r(S, \theta)$ is the pressure that a parcel would have in its reference position. It therefore represents a generalised form of potential density, which as it turns out is more neutral than any standard form of potential density. As a result, inferring information about the diapycnal diffusivities from global budgets or inverse methods requires being able to disentangle the part of the effective diffusivity that is controlled by isoneutral mixing. The idea that the effective diffusivity might be contaminated to some degree by isoneutral mixing was hypothesised by Lee et al. (2002), but they assumed the effect to be second order and made no attempt at quantifying it. The present results suggest the effect might in fact be more important than usually assumed and therefore warranting more attention that it has usually received. Another motivation for the present study stems from a recent isopycnal justification for the well-known one-dimensional advection/diffusion model for ocean heat uptake in which the diapycnal diffusivity diffusing heat downward is the effective diapycnal diffusivity discussed in the present paper, see <https://arxiv.org/abs/1708.02085>.

The main goal of the present paper is to assess the above mentioned effect in details, which we believe is done here for the first time. For the sake of clarity, the directions parallel and perpendicular to the local neutral tangent planes are referred to as 'diapycnal' and 'isopycnal' respectively, the terms 'diapycnal' and 'isopycnal' being used when isopycnal surfaces are defined in terms of a material density variable $\gamma(S, \theta) = \text{constant}$. To that end, we seek to quantify the degree of contamination of estimates of diapycnal mixing by isoneutral mixing for a number of density variable of the form $\gamma(S, \theta)$, illustrated for the following five density variables: Jackett and McDougall (1997) γ^n , three potential density variables $\sigma_0, \sigma_2, \sigma_4$ and the Lorenz reference state density ρ_{ref} . Note that although ω surfaces Klocker et al. (2009) are more neutral than γ^n , they are likely to

be less material (a material density variable is a variable conserved whenever θ and S are both conserved i.e. a function of θ and S only) because improved neutrality tends to occur at the expense of materiality. Moreover, no density variable associated with ω -surfaces has been constructed yet, which makes the use of the latter impractical for the present purposes. These density variables have been chosen because they are widely used in the oceanographic community and thus deserve special attention.

- 5 **Note, however, that γ^n is not a function of (θ, S) alone, but also depends on latitude, longitude and pressure, which means that it is not fully material; nevertheless, its degree of non-materiality is generally assumed to be small (see McDougall and Jackett (2005)).** Section 2 presents the theoretical framework used for defining effective diffusivities for each variable. Section 3 discusses the results obtained for the above mentioned 5 density variables. Finally, Section 4 summarises and discusses the results.

10 2 Method

2.1 Effective diffusivity

Thermodynamic properties in numerical ocean models are commonly formulated in terms of θ and S , whose evolution equations can in general be expressed as:

$$\frac{D_{\text{res}}\theta}{Dt} = \nabla \cdot (\mathbf{K}\nabla\theta) + f_\theta, \quad \frac{D_{\text{res}}S}{Dt} = \nabla \cdot (\mathbf{K}\nabla S) + f_S, \quad (9)$$

- 15 where $\mathbf{K} = K_i(\mathbf{I} - \mathbf{d} \cdot \mathbf{d}^T) + K_d\mathbf{d} \cdot \mathbf{d}^T$ is Redi (1982)'s neutral rotated diffusion tensor (with K_i and K_d being the isoneutral and dianeutral turbulent mixing coefficients respectively, $\mathbf{d} = \mathbf{N}/|\mathbf{N}|$ the locally-defined normalised neutral vector), f_S, f_θ respectively the forcing terms for salinity and potential temperature and $D_{\text{res}}/Dt = \partial/\partial t + (\mathbf{v} + \mathbf{v}_{gm}) \cdot \nabla$ the advection by the residual velocity (the sum of the resolved Eulerian velocity plus the meso-scale eddy induced velocity). Note here that K_i and K_d are implicitly defined in terms of the orthogonal projections of the turbulent heat and salt fluxes on the isoneutral and dianeutral directions; for an alternative and more recent definition of K_i and K_d aimed at making dianeutral mixing appear to be isotropic, see McDougall et al. (2014). The evolution equation of any material density variable $\gamma(S, \theta)$ must be given

$$\frac{D_{\text{res}}\gamma}{Dt} = \nabla \cdot (\mathbf{K}\nabla\gamma) - \underbrace{(\gamma_{\theta\theta}\nabla\theta^T\mathbf{K}\nabla\theta + 2\gamma_{S\theta}\nabla S^T\mathbf{K}\nabla\theta + \gamma_{SS}\nabla S^T\mathbf{K}\nabla S)}_{NL}. \quad (10)$$

Unless $\gamma(S, \theta)$ is a linear function of S and θ , its evolution equation will in general contain non vanishing nonlinear terms (denoted NL in Eq. (10)) related to cabelling and thermobaricity, e.g., McDougall (1987b); Klocker and McDougall (2010);

- 25 Urakawa et al. (2013). The diffusive flux of γ is:

$$F_{\text{diff}}^\gamma = -\mathbf{K}\nabla\gamma = \underbrace{-K_i(\nabla\gamma - (\nabla\gamma \cdot \mathbf{d})\mathbf{d})}_{F_{\text{diff}}^i} - \underbrace{K_d(\nabla\gamma \cdot \mathbf{d})\mathbf{d}}_{F_{\text{diff}}^d} \quad (11)$$

Where F_{diff}^i and F_{diff}^d are respectively the diffusive flux of γ in the isoneutral and dianeutral direction. For clarity, figure 1 shows a schematic of the neutral plane, of the $\gamma = \text{const.}$ plane, of the $\nabla\gamma$ and neutral direction and of F_{diff}^i and F_{diff}^d .

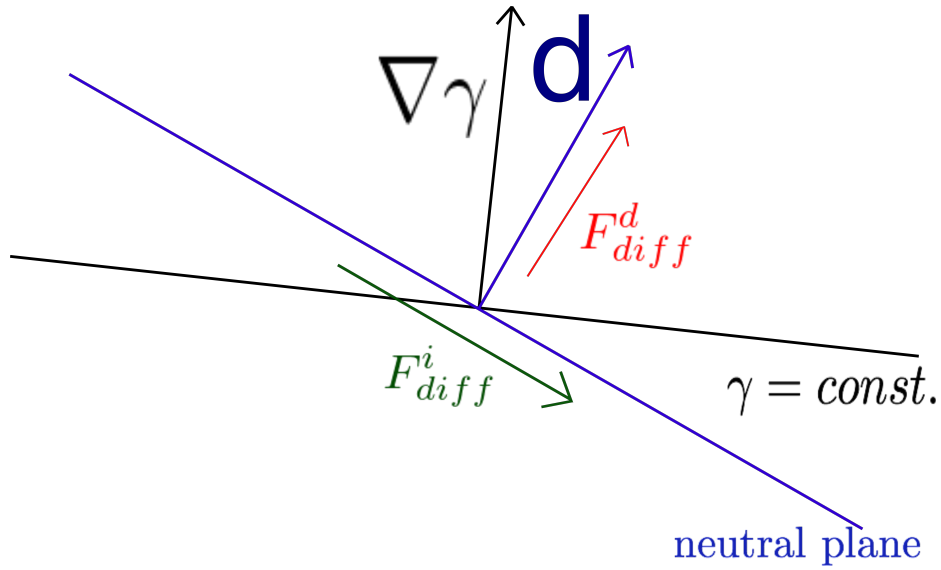


Figure 1. Schematic showing the neutral plane and neutral direction \mathbf{d} in blue, the $\gamma = \text{const.}$ plane and $\nabla\gamma$ direction in black and the projection of the diffusive flux of γ in the isoneutral (F_{diff}^i) and dianeutral (F_{diff}^d) direction.

We define the effective diffusive flux of γ as the integral of the diffusive flux across the isopycnal surface $\gamma(\mathbf{x}, t) = \text{constant}$, viz.,

$$F_{\text{eff}} = - \int_{\gamma=\text{const}} \mathbf{K} \nabla\gamma \cdot \mathbf{n} dS \quad (12)$$

where $\mathbf{n} = \frac{\nabla\gamma}{|\nabla\gamma|}$ is the unit local normal vector to the γ surface. Now, it is easily established after some straightforward algebra

5 that

$$\begin{aligned} \mathbf{K} \nabla\gamma \cdot \mathbf{n} &= [K_i (\nabla\gamma - (\nabla\gamma \cdot \mathbf{d}) \mathbf{d}) + K_d (\nabla\gamma \cdot \mathbf{d}) \mathbf{d}] \cdot \frac{\nabla\gamma}{|\nabla\gamma|} \\ &= [K_i (|\nabla\gamma|^2 - (\nabla\gamma \cdot \mathbf{d})^2) + K_d (\nabla\gamma \cdot \mathbf{d})^2] / |\nabla\gamma| \\ &= |\nabla\gamma| [K_i \sin^2(\nabla\gamma, \mathbf{d}) + K_d \cos^2(\nabla\gamma, \mathbf{d})]. \end{aligned} \quad (13)$$

Eq. (13) establishes that the locally defined effective diapycnal diffusivity experienced by the density variable γ is affected by both isoneutral and dianeutral mixing, the contribution from isoneutral mixing being akin to a Veronis-like effect, as discussed in Tailleux (2016b). Because we are primarily interested in the latter effect, we shall discard the effect of dianeutral mixing on the effective diapycnal diffusivity of γ and hence assume $K_d = 0$ in the rest of the paper. As a result, the expression for the effective diffusive flux of γ becomes:

$$F_{\text{eff}} = - \int_{\gamma=\text{const}} |\nabla\gamma| K_i \sin^2(\nabla\gamma, \mathbf{d}) dS. \quad (14)$$

Note that the integrand of (14) is mathematically equivalent to what McDougall and Jackett (2005) refer to as “fictitious diapycnal mixing”. However, here the integrand is integrated on γ surfaces and then used to calculate an effective diffusivity coefficient which is easier to interpret than a collection of local values of the $(\nabla\gamma, \mathbf{d})$ angle.

2.2 Reference Profile

- 5 In order to construct an effective turbulent diffusivity K_{eff} associated with the effective diffusivity flux F_{eff} , we need to define an appropriate mean gradient for the density variable γ . This is done by constructing a reference profile for γ , as explained in the next paragraph.

Let $z_r(\gamma, t)$ be the reference profile for the particular material density $\gamma(S, \theta)$ (which can always be written as a function of space \mathbf{x} and time t as $\gamma^*(\mathbf{x}, t) = \gamma(S, \theta)$), constructed to be the implicit solution of the following problem:

$$10 \quad \int_{V(z_r)} dV = \int_{V(\gamma, t)} dV = \int_{z_r(\gamma, t)}^0 A(z) dz, \quad (15)$$

where $A(z)$ is the depth-dependent area of the ocean at depth z , and $V(\gamma, t)$ the volume of water for all parcels with density γ_0 such that $\gamma_{\min} \leq \gamma_0 \leq \gamma$, where γ_{\min} is the minimum value of γ encountered in the ocean. The knowledge of the reference profile allows one to regard the volume $V(\gamma, t)$ of water masses with density lower than γ either as a function of z_r only as $V(z_r)$ so that $V(\gamma, t) = V(z_r(\gamma, t))$. Physically, Eq. (15) defines the reference depth $z_r(\gamma, t)$ so that the volume of water with

- 15 density lower than γ is equal to the volume of water comprised between the ocean surface and z_r ; this definition is equivalent to that used by Winters and D’Asaro (1996) or Saenz et al. (2015) to construct the Lorenz reference state, but generalised here to the case of an arbitrary materially conserved density variable $\gamma(S, \theta)$. Once $z_r(\gamma, t)$ is constructed, it can be inverted to define in turn the reference profile $\gamma_r(z_r, t)$. Indeed, by definition $\gamma_r(z_r(\mathbf{x}, t), t) = \gamma^*(\mathbf{x}, t)$. As a result, we can always write a relation such as:

$$20 \quad \nabla\gamma = \frac{\partial\gamma_r}{\partial z_r} \nabla z_r \quad (16)$$

A major difference with Winters and D’Asaro (1996) or Griffies et al. (2000) is that our definition of reference depth and density is not restricted to Lorenz reference state, for it can be applied to any arbitrary $\gamma(S, \theta)$. However, the choice of $\gamma(\theta, S)$ influences the local projection of the iso-dianeutral diffusion on the γ gradient and thus the effective diapycnal coefficient. We now define the effective diffusivity K_{eff} . Using (16) in (14), we get:

$$25 \quad F_{\text{eff}} = - \int_{\gamma=\text{const}} |\nabla\gamma| K_i \sin^2(\nabla\gamma, \mathbf{d}) dS = \frac{\partial\gamma_r}{\partial z_r} \int_{z_r=\text{const}} |\nabla z_r| K_i \sin^2(\nabla z_r, \mathbf{d}) dS = A(z_r) K_{\text{eff}} \frac{\partial\gamma_r}{\partial z_r}, \quad (17)$$

where we have used $|\nabla\gamma| = -\frac{\partial\gamma_r}{\partial z_r} |\nabla z_r|$ (because $\frac{\partial\gamma_r}{\partial z_r} < 0$) and where K_{eff} is defined by the following relation:

$$K_{\text{eff}}(z_r) = \frac{\int_{z_r=\text{const}} K_i |\nabla z_r| \sin^2(\nabla z_r, \mathbf{d}) dS}{A(z_r)}, \quad (18)$$

and is independent of the gradient of γ_r in the reference space. K_{eff} is not the surface average of the local mixing coefficient across $\gamma = \text{const.}$ surfaces but rather the mixing coefficient linked to the time variation of γ_r as can be seen from the following equation (a proof is shown in the appendix):

$$\frac{\partial \gamma_r}{\partial t} = \frac{1}{A(z_r)} \frac{\partial}{\partial z_r} \left(A(z_r) K_{\text{eff}}(z_r) \frac{\partial \gamma_r}{\partial z_r} \right) + \text{NL} + F, \quad (19)$$

- 5 where NL is a term due to the non linearity of $\gamma(S, \theta)$ and F is a term due to the heat and haline fluxes at the ocean surface. Note that in Speer (1997) and in Lumpkin and Speer (2007), the effective diffusivity is defined as the integral of the local diapycnal flux on a γ surface over the integral of the local gradient of γ on the same γ surface i.e.:

$$K_{\text{eff}}^{\text{speer}} = \frac{\int_{z_r=\text{const}} K \nabla \gamma \cdot \mathbf{n} dS}{\int_{z_r=\text{const}} \nabla \gamma \cdot \mathbf{n} dS}, \quad (20)$$

- this** is different from our formulation because of the different mean gradient formulation. The relationship between the K_{eff} described in this article (a generalization of Winters and D'Asaro (1996)'s formulation) and $K_{\text{eff}}^{\text{speer}}$ is, from formula (18) and (20):

$$K_{\text{eff}} = K_{\text{eff}}^{\text{speer}} \left(\frac{\int_{z_r=\text{const}} |\nabla z_r| dS}{A(z_r)} \right). \quad (21)$$

- We have checked that for all the density variables under consideration here the quantity between brackets in (21) is smaller than 1 so that K_{eff} can be seen as a lower bound of $K_{\text{eff}}^{\text{speer}}$. In Lee et al. (2002), the effective diapycnal coefficient formulation is similar to Speer (1997)'s except that the mean gradient is approximated by an average of the vertical gradient of γ on a γ surface which is valid as long as the γ slope is small.

3 Isoneutrally-controlled effective diapycnal diffusivities for σ_0 , σ_2 , σ_4 , γ^n and ρ_{ref}

- In this section we seek to estimate the effective diffusivity (18) derived in the previous section for five different density variables: σ_0 , σ_2 , σ_4 , the Jackett and McDougall (1997)'s γ^n and the Lorenz reference density ρ_{ref} obtained with Saenz et al. (2015) method. All the calculations of this section are performed with annual mean potential temperature and salinity data from the World Ocean Circulation Experiment (Gouretski and Koltermann, 2004). Since γ^n is not well defined North of 60° N, the latter region was excluded from our analysis for all five density variables. Since eddies mix the fluid horizontally in the mixed layer rather than perpendicular to the neutral vector, we also restrict our calculation to the ocean below the mixed layer. The depth of the mixed layer is given by the de Boyer Montégut database (de Boyer Montégut et al., 2004). The reference density for each of the five variables is shown on figure 2. As expected, the range of values taken by the reference density of the three potential density variables increases with the reference pressure. γ^n has a reference density similar to that of σ_0 with a slightly smaller gradient in the reference space. ρ_{ref} has a gradient much **larger** ~~smaller~~ than all other density variables. It crosses σ_0 at the surface, σ_2 around -2000 meters and σ_4 around -4000 meters. This is due to the fact that the volume above the surface $\sigma_p(\theta, S) = \sigma_p^r(Z)$ is by definition the same as the volume above $\rho(\theta, S, p) = \rho_{ref}(Z)$ where $p = -Z\rho_0g$ is

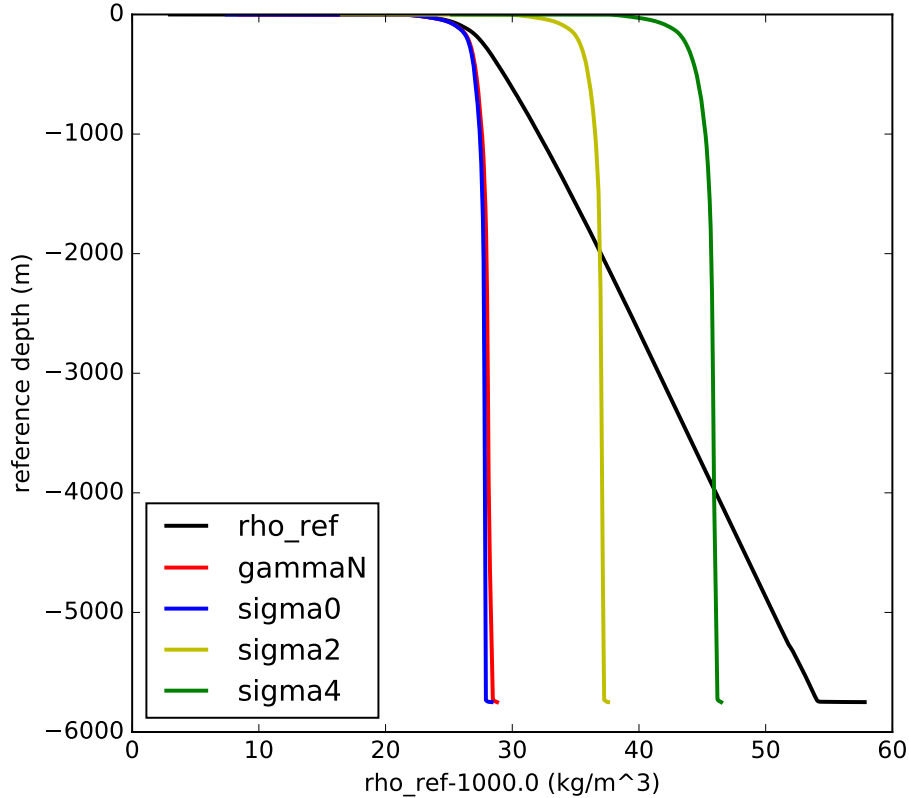


Figure 2. Reference density for ρ_{ref} (black) γ^n (red), σ_0 (blue), σ_2 (yellow) and σ_4 (green) as a function of the reference depth.

the reference pressure linked to the reference depth Z , σ_p^r is the reference density linked to σ_p .

Figure 3 shows the histogram of the decimal logarithm of the squared sine of the angle between $\nabla\gamma$ and \mathbf{d} (calculated using formula A1) shown in appendix A): $\log_{10}[\sin(\nabla\gamma, \mathbf{d})]$ and weighted by the volume associated with each point. This plot is similar to that discussed by McDougall and Jackett (2005) in their discussion of fictitious diapycnal mixing.

- 5 ρ_{ref} , σ_2 and σ_4 give similar angles with most of their values slightly larger than 10^{-5} . γ^n gives the smallest angles among the variables under consideration here with most of its values smaller than 10^{-5} while σ_0 gives the largest with a large number of points with values larger than 10^{-4} . All together, these observations could suggest that the effective diffusivity of γ^n should be the smallest overall, that the effective diffusivity of ρ_{ref} should be of the same order as that for σ_2 and σ_4 , and that the effective diffusivity for σ_0 should be the largest of all. It is however hard to predict the values of the effective diffusivity coefficient
- 10 for each density variable from figure 3 only since the small number of point with very large angle values (hardly visible on figure 3) could dominate the large number of points with small angles and since the spatial variability of the isoneutral mixing coefficient could correlates with the spatial variability of the angle. We thus calculate the effective diffusivity coefficient using

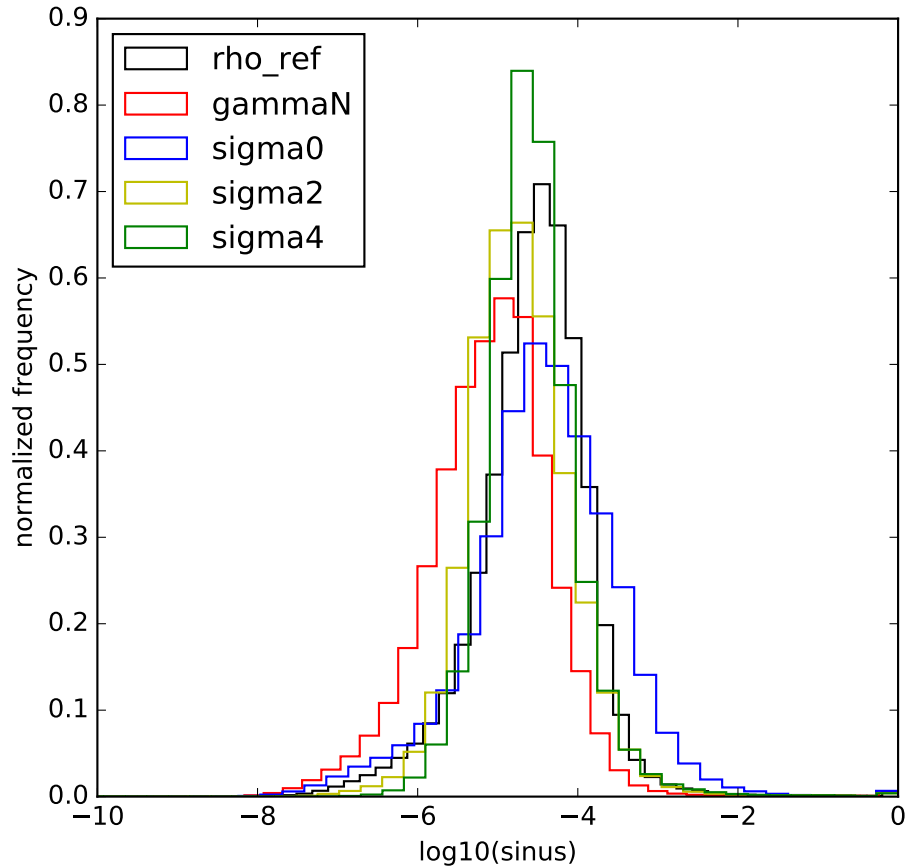


Figure 3. histogram of the decimal logarithm of the squared sine between the gradient of γ and the neutral vector \mathbf{d} weighted by the volume of each point. $\log_{10}(\sin(\nabla\gamma, \mathbf{d}))$ for ρ_{ref} (black), γ^n (red), σ_0 (blue), σ_2 (yellow) and σ_4 (green)

these angles values for each density variable.

Figure 4 shows the decimal logarithm of the effective diffusivity K_{eff} for the five variables as a function of the reference depth under two possible choices of K_i :

5

The first case (A, figure 4) assumes a constant isoneutral coefficient: $K_i = 1000 \text{ m}^2/\text{s}$. Under this assumption, K_{eff} for every density variables increases on average with the reference depth from values between 10^{-12} and $10^{-8} \text{ m}^2/\text{s}$ close to surface reference depth to values between 10^{-6} and $0 \text{ m}^2/\text{s}$ at the deepest reference depths. This increase can be attributed to the fact that the largest discrepancy between the neutral vector and the gradients of the 5 density variables is generally located in the ACC (Antarctic Circumpolar Current) (as will be shown later) where the highest densities, and thus deepest reference depths,

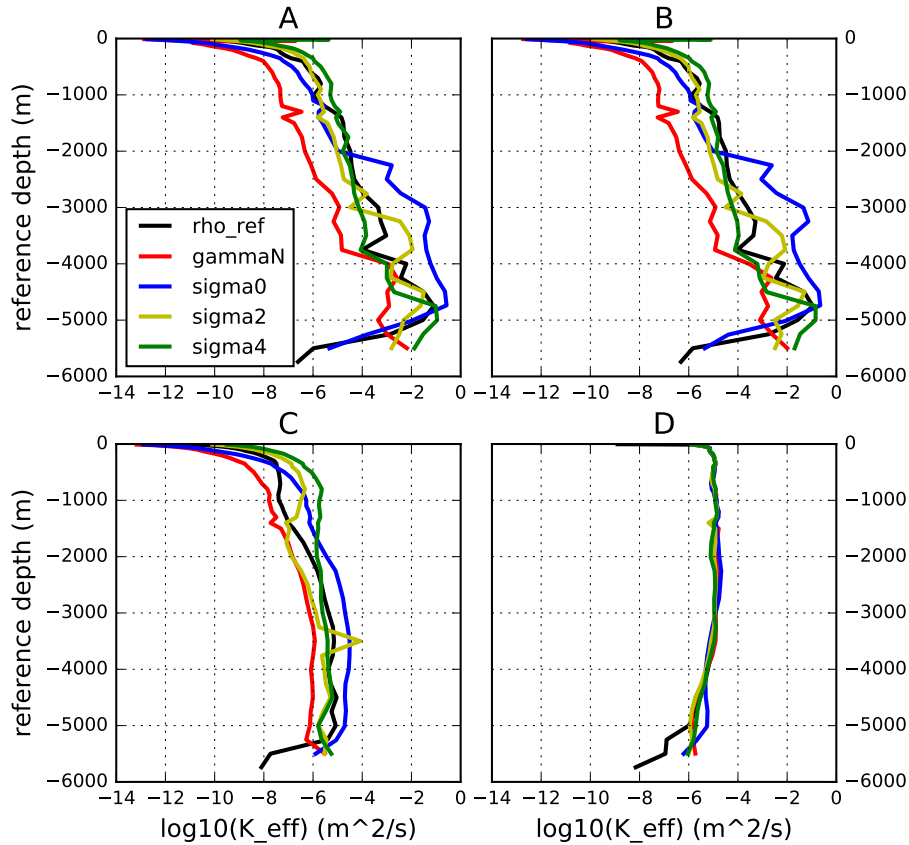


Figure 4. \log_{10} of the effective diapycnal diffusivity coefficient K_{eff} as a function of the reference depth (meters) (and as defined by equation (18)) for ρ_{ref} (black), γ^n (red), σ_0 (blue), σ_2 (yellow) and σ_4 (green). Panels A,B and C correspond to a K_{eff} calculated with different isoneutral diffusivity coefficient. A: $K_{\text{iso}} = 1000 \text{ m}^2/\text{s}$, B: variable isoneutral diffusivity coefficient given by Forget et al. (2015). C: same as B but without 5% of the largest angles. **Bottom right, D:** $\log_{10} K_{\text{eff}}$ calculated from a variable diapycnal diffusivity coefficient given by the inverse calculation of Forget et al. (2015).

outcrop.

K_{eff} for γ^n and σ_0 are similar between 0 and 800 m depth with values ranging from $10^{-8} \text{ m}^2/\text{s}$ at the surface to $10^{-6} \text{ m}^2/\text{s}$ at -800 meters. σ_2 , σ_4 and ρ_{ref} give values up to 100 larger on the same depth range. Between 800 and 4000 m depth, γ^n gives the smallest K_{eff} which is slowly increasing from 10^{-6} to $10^{-5} \text{ m}^2/\text{s}$ as the depth decreases. On the same depths, ρ_{ref} , σ_0 , σ_2 and σ_4 gives values at least 10 times larger (up to 1000 times larger for σ_0 below -2000 m). Below 4000 m depth, all density variables have a K_{eff} larger than $10^{-4} \text{ m}^2/\text{s}$ (note that $10^{-4} \text{ m}^2/\text{s}$ is the widely cited Munk (1966) and Munk and Wunsch (1998)'s canonical estimate of diapycnal mixing inferred from the global heat and mechanical energy budgets.) At the deepest levels, under -5000 meters, σ_0 and ρ_{ref} have a smaller K_{eff} than γ^n suggesting that their local gradients are very nearly aligned

with the neutral vector at these deep reference depths.

The second case (B, figure 4) assumes a spatially variable isoneutral coefficient given by the inverse calculation of Forget et al. (2015), which gives a three dimensional distribution of K_i at about 1° resolution for the global ocean. This database contains values ranging from $9000 \text{ m}^2/\text{s}$ (in the Atlantic deep water formation zone at the surface, in western boundary currents and ACC) to values close to 0 (in the deep pelagic ocean). The estimated K_{eff} for this choice are very close to those obtained under the previous assumption of constant diffusivity for all variables, showing the small sensitivity of our results to spatial variations of isoneutral diffusion, which is further discussed below.

To investigate the importance of the localised large departure from neutrality in the construction of K_{eff} , we removed 5% of the largest non-neutral values of the angle for each reference surface (figure 4, case C). Without 5% of the largest values, K_{eff} is much smaller than the previous one for every density variables with values everywhere smaller than $10^{-4} \text{ m}^2/\text{s}$. As before, the effective diffusivity increases rapidly close to the surface and then more slowly below -1000 meters (except at a few depth for σ_2 , σ_4 and at deep reference depth for ρ_{ref} and σ_0) with the reference depth for all density variables. γ^n gives the smallest values for almost all reference depths, with values from $10^{-10} \text{ m}^2/\text{s}$ close to the surface of the reference space to $10^{-6} \text{ m}^2/\text{s}$ at the deepest levels. σ_2 gives the second smallest values for reference depths smaller than -1500 meters but is overtaken by σ_0 and ρ_{ref} at larger depths. $\rho_{ref}, \sigma_0, \sigma_2$ and σ_4 all give effective diffusivities of the order or larger than $10^{-5} \text{ m}^2/\text{s}$ at some depth below -2000 meters.

This calculation shows that the isoneutral contribution to effective diapycnal mixing is very localised spatially with 5% of each surface accounting for most of the effective diffusivity for all the density variables under consideration here. However, even without this top 5%, K_{eff} remains close or above $10^{-5} \text{ m}^2/\text{s}$ for all variables except γ^n . Coming back to the similarity between panels A and B, the location of the top 5% values are correlated with local K_i values (from Forget et al. (2015) database) around $1000 \text{ m}^2/\text{s}$ which therefore explain the lack of sensitivity of our results on the choice of K_i between A and B.

Panel D shows K_{eff} calculated using a dianeutral mixing coefficient given by Forget et al. (2015) inverse calculation assuming no isoneutral mixing. The formula for this calculation is obtained by replacing the sine by a cosine and K_i by K_d in formula (18) following formula (13), i.e. :

$$K_{\text{eff}}(z_r) = \frac{\int_{z_r=\text{const}} K_d |\nabla z_r| \cos^2(\nabla z_r, \mathbf{d}) dS}{A(z_r)}. \quad (22)$$

K_{eff} values are smaller or close to $10^{-5} \text{ m}^2/\text{s}$ at all reference depths for all density variables. For reference depth deeper than 1000 meters, these values are much smaller than the effective diffusivity estimated from the isoneutral mixing coefficient as shown on panel A or B. Without the 5% of the largest values on each density surface, K_{eff} estimated from variable K_i (panel C) is smaller than the one estimated from variable K_d for all density variables above 1000 meters. The exception is γ^n which gives K_{eff} estimated from K_i approximately 10 times smaller than K_{eff} from K_d at all reference depths below 1000 m. Note that the values obtained from the dianeutral coefficient are much less sensitive to the choice of density variable than the values obtained from the isoneutral mixing coefficient. This is because of the 7 order of magnitude difference between K_d and K_i which makes the K_{eff} estimated from the isoneutral coefficient much more sensitive to the angle between the neutral vector and the local gradient of the density variable under consideration.

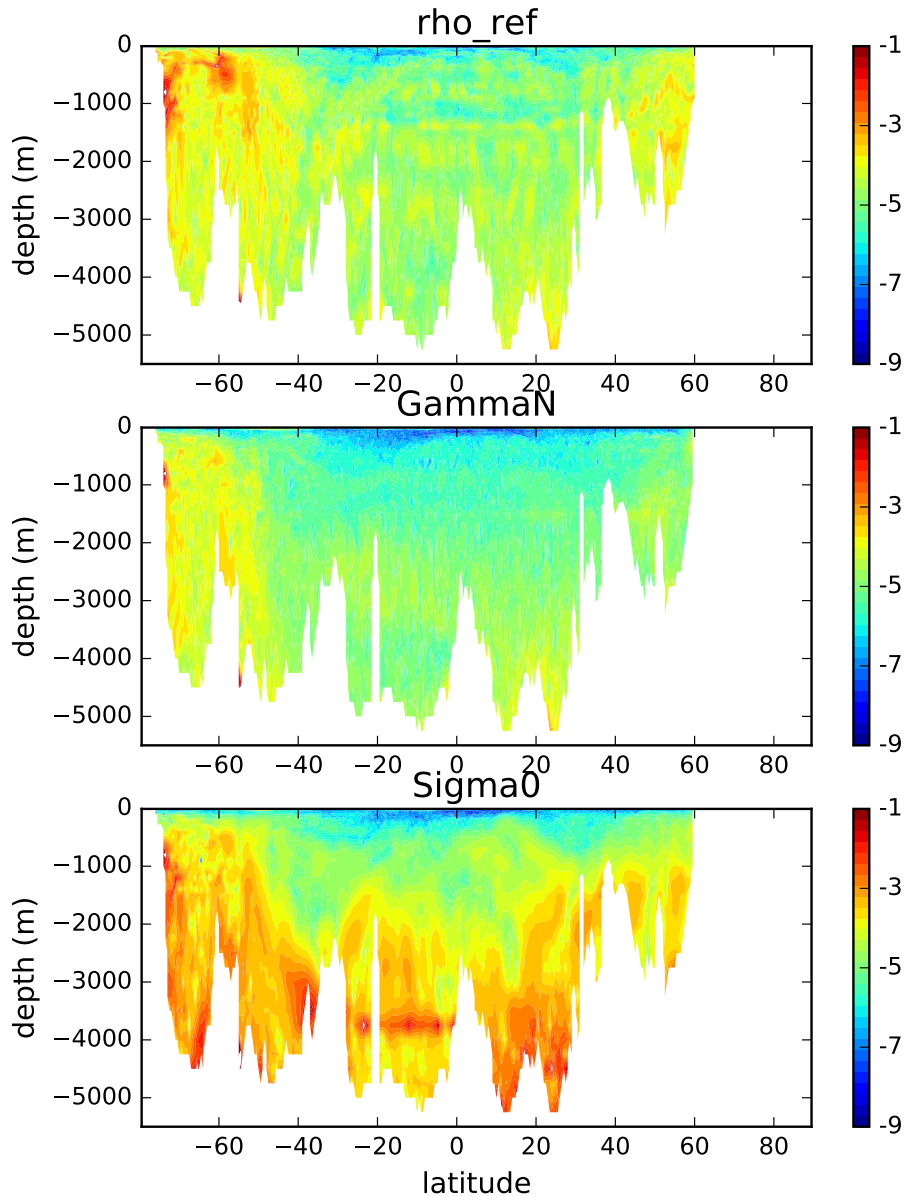


Figure 5. Decimal logarithm of the sine between the neutral vector and the gradient of ρ_{ref} (top), γ^n (middle) and σ_0 (bottom) as a function of latitude and depth at 330 of longitude (in the Atlantic).

Figure 5 shows a meridional section of the decimal logarithm of the sine in the Atlantic for ρ_{ref} , γ^n and σ_0 . The regions where the angle between the neutral vector and the gradient of the density variable is large are found mostly in the ACC at all depth for ρ_{ref} and γ^n and everywhere at depth for σ_0 , suggesting that, in this region, all the density variables studied above

introduce significant biases in the estimation of diapycnal mixing.

4 Conclusions

In this paper, we have presented a new framework for assessing the contribution of isoneutral diffusion to the effective diapycnal mixing coefficient K_{eff} for five different density variables, chosen for their widespread use in the oceanographic community, namely $\gamma^n, \rho_{ref}, \sigma_0, \sigma_2, \sigma_4$. Our results reveal that, due to the projection of the isoneutral mixing on the diapycnal direction, the actual diapycnal mixing experienced by each density variable can reach values as high as $10^{-4} \text{ m}^2/\text{s}$ and up to $0.1 \text{ m}^2/\text{s}$ for reference depths deeper than 2000 meters. **These values are generally 10 to 100 times larger below -1000m and up to 1000 times larger below -4000 meters than the ones estimated from a variable dianeutral coefficient which are always around or below $10^{-5} \text{ m}^2/\text{s}$.**

As expected, γ^n , constructed to be as neutral as practically feasible, is the least affected by isoneutral diffusion of all density variables considered. Nevertheless, it still appears to experience values larger than $10^{-4} \text{ m}^2/\text{s}$ for reference depths below -4000 meters i.e. 10 to 100 times larger than the corresponding values obtained assuming a variable dianeutral. Note that an added difficulty pertaining to the use of γ^n , stems from its non-material character. As a result, the validity of defining an effective diapycnal diffusivity for γ^n using the present approach depends on such non-material effects to be small, or at least much smaller than the contribution from isopycnal diffusion discussed here, which is difficult to evaluate.

Our results thus suggest that the potential contamination due to isoneutral mixing should always be assessed for any inference of diapycnal mixing based on the use of any density variable $\gamma(S, \theta)$ in Walin-like water mass analysis for instance. In agreement with previous studies such as McDougall and Jackett (2005), the regions of large discrepancy between the neutral vector and the gradient of each surface are very localised in space. However, while representing a very small amount of volume of the ocean, these discrepancies are important in setting the effective diffusivity values. Indeed, without 5% of the largest angle values between the neutral vector and the local γ gradient, none of the variables gives a coefficient larger than $10^{-4} \text{ m}^2/\text{s}$. **Moreover, the estimated values are everywhere comparable or smaller than the coefficient estimated from dianeutral mixing only.** The concentration of discrepancies is even stronger for γ^n since the effective diffusivity coefficient after the removal of the 5% of the largest values decreases below $10^{-6} \text{ m}^2/\text{s}$. **Overall, the K_{eff} profiles for each density variables become similar without the 5% suggesting that the choice of the density variable is less important when the Southern ocean (which is where most of the largest discrepancies between neutral and local γ gradient are located) is not taken into account.**

However, when no part of the ocean is removed (as it is the case in Walin (1982) type calculation for instance), the effective diffusivities found in this article are very sensitive to the density variable under consideration. This is at odd with the results of Megann (2018) and could suggest that their effective diffusivities are mainly driven by spurious numerical mixing.

Our results show that the evaluation of effective diapycnal mixing using a sorting algorithm of density (e.g. Griffies et al. (2000); Ilıcak et al. (2012)), which amounts to diagnosing the diapycnal flux through ρ_{ref} , is likely to be significantly contaminated by isoneutral diffusion owing to the large departures from neutrality of ρ_{ref} in the polar regions if a nonlinear equation of state

is used. Note that this is a distinct effect from the density sinks and sources due to the non-linear equation of state influencing the time variation of the reference density (see equation (19)) which are also a source of contamination of the diapycnal flux from the isoneutral diffusion when using sorting algorithm. It follows that diagnosing the spurious diapycnal mixing resulting from numerical advection schemes for a nonlinear equation of state remains an outstanding challenge, and that progress on this

5 topic must take into account the theoretical considerations developed here. This work advocates for the construction of a density function $\gamma(\theta, S)$ that would minimize the isoneutral influence on the effective diapycnal diffusivity coefficient. So far, the best material density variable is a function of Lorenz reference density, as shown by Tailleux (2016a), but as discussed by Tailleux (2016b), it appears theoretically possible to construct an even more neutral one. Whether Klocker et al. (2009) can be used for global inversions is unclear, because its improved neutrality might

10 be achieved at the expenses of materiality, which remains to be quantified. In theories of the Atlantic Meridional Overturning Circulation (AMOC) (e.g. Vallis (2000); Wolfe and Cessi (2010); Nikurashin and Vallis (2011, 2012)) the diapycnal diffusion coefficient is generally assumed to be given by the dianeutral coefficient and to be of the order of $10^{-5} \text{ m}^2/\text{s}$. However, our results suggest that even when isopycnals are given by a density variable close to the neutral vector (e.g. with γ^n), the effective diapycnal coefficient can be much larger than the dianeutral coefficient because

15 of the isoneutral diffusion. The issue of the amount of diapycnal mixing is an important one, as illustrated for instance by Nikurashin and Vallis (2012) who showed that low and large diapycnal coefficient give two different regimes of the AMOC and thus possibly two different evolution under climate change. Obviously this effect appears only when the equation of state for density is a non-linear function of both temperature and salinity we thus argue that future work should consider such non-linear equation of state for density.

20 **Appendix A: Numerical calculation of $\sin(\nabla\gamma, \mathbf{d})$**

To calculate the numerical value of $\sin(\nabla\gamma, \mathbf{d})$ we use the cross product between $\nabla\gamma$ and \mathbf{d} :

$$|\sin(\nabla\gamma, \mathbf{d})| = \frac{|\nabla\gamma \times \mathbf{d}|}{|\nabla\gamma|} \quad (\text{A1})$$

where \times is the cross product. This method can be used with all the variables studied here since it only requires the knowledge of $\gamma(S, \theta)$. In practice, \mathbf{d} is specified as the normalised neutral vector $\mathbf{d} = \mathbf{N}/|\mathbf{N}|$.

25 **Appendix B: equation (19)**

The evolution equation for γ is:

$$\frac{d\gamma}{dt} = \frac{\partial\gamma}{\partial\theta} \frac{d\theta}{dt} + \frac{\partial\gamma}{\partial S} \frac{dS}{dt} = \frac{\partial\gamma}{\partial\theta} \nabla(K\nabla\theta) + \frac{\partial\gamma}{\partial S} \nabla(K\nabla S) + \frac{\partial\gamma}{\partial\theta} f_\theta + \frac{\partial\gamma}{\partial S} f_S \quad (\text{B1})$$

$$= \nabla(K\nabla\gamma) - K\nabla\theta \cdot \nabla \left(\frac{\partial\gamma}{\partial\theta} \right) - K\nabla S \cdot \nabla \left(\frac{\partial\gamma}{\partial S} \right) + f_\gamma \quad (\text{B2})$$

where f_θ , f_S are the surface heat and haline fluxes and where $f_\gamma = \frac{\partial \gamma}{\partial \theta} f_\theta + \frac{\partial \gamma}{\partial S} f_S$. Then let $z_r(X, t)$ be the reference level of γ defined by equation (15) so that γ can now be written: $\gamma(S, \theta) = \gamma_r(z_r, t)$. Then integrating (B2) on a volume $V(z_r)$ defined by water parcels of reference level larger than or equal to z_r gives:

$$\int_{V(z_r)} \frac{\partial \gamma}{\partial t} dV + \gamma_r(z_r, t) \int_{z_r=\text{const}} \mathbf{u} \cdot \mathbf{n} dS = \int_{z_r=\text{const}} K \nabla \gamma \cdot \mathbf{n} dS - \int_{V(z_r)} K \nabla \theta \cdot \nabla \left(\frac{\partial \gamma}{\partial \theta} \right) + K \nabla S \cdot \nabla \left(\frac{\partial \gamma}{\partial S} \right) dV + \int_{V(z_r)} f_\gamma dV \quad (\text{B3})$$

- 5 where $z_r = \text{const}$ refers to the constant z_r surface. $\mathbf{n} = \frac{\nabla \gamma}{|\nabla \gamma|} = -\frac{\nabla z_r}{|\nabla z_r|}$ is the local normal to the surface $\gamma = \text{const}$, the minus sign arises because the integration is done toward deeper values of z_r . The second term on the left hand side is zero because of the non-divergence of the velocity and the first term can be written as:

$$\int_{V(z_r)} \frac{\partial \gamma}{\partial t} dV = \frac{\partial}{\partial t} \int_{V(z_r)} \gamma_r dV' - \underbrace{\gamma_r \frac{\partial V(z_r)}{\partial t}}_{=0} \quad (\text{B4})$$

- The second term on the right hand side is zero because the total volume at constant z_r is independent of time (see formula 10 (15)). Using (B4) and the z_r derivative of (B3) we get:

$$\frac{\partial \gamma_r}{\partial t} = \frac{1}{A(z_r)} \frac{\partial}{\partial z_r} \left(A(z_r) K_{\text{eff}}(z_r) \frac{\partial \gamma_r}{\partial z_r} \right) + \text{NL} + \text{forcing} \quad (\text{B5})$$

where we have used formula (15) and the fact that the volume integral of a z_r only function can be expressed as an integral over the reference depth:

$$\frac{\partial}{\partial z_r} \left(\frac{\partial}{\partial t} \int_{V(z_r)} \gamma_r dV' \right) = \frac{\partial}{\partial t} \left(\frac{\partial}{\partial z_r} \int_{z_r}^0 A(z'_r) \gamma_r(z'_r, t) dz'_r \right) = -A(z_r) \frac{\partial \gamma_r}{\partial t} \quad (\text{B6})$$

- 15 and with:

$$\text{NL} = \frac{1}{A(z_r)} \frac{\partial}{\partial z_r} \left(\int_{V(z_r)} \left(K \nabla \theta \cdot \nabla \left(\frac{\partial \gamma}{\partial \theta} \right) + K \nabla S \cdot \nabla \left(\frac{\partial \gamma}{\partial S} \right) \right) dV \right) \quad (\text{B7})$$

and

$$\text{forcing} = -\frac{1}{A(z_r)} \frac{\partial}{\partial z_r} \left(\int_{V(z_r)} f_\gamma dV \right) \quad (\text{B8})$$

and finally K_{eff} given by formula (18).

- 20 *Acknowledgements.* This work was supported by the grant NE/K016083/1 ‘‘Improving simple climate models through a traceable and process-based analysis of ocean heat uptake (INSPECT)’’ of the UK Natural Environment Research Council (NERC). Modeling results presented in this study are available upon request to the corresponding author.

References

- de Boyer Montégut, C., Madec, G., Fischer, A. S., Lazar, A., and Iudicone, D.: Mixed layer depth over the global ocean: An examination of profile data and a profile-based climatology, *Journal of Geophysical Research: Oceans*, 109, 2004.
- Forget, G., Ferreira, D., and Liang, X.: On the observability of turbulent transport rates by Argo: supporting evidence from an inversion experiment, *Ocean Science*, 11, 839, 2015.
- Gouretski, V. and Koltermann, K. P.: WOCE global hydrographic climatology, *Berichte des BSH*, 35, 1–52, 2004.
- Griffies, S. M., Pacanowski, R. C., and Hallberg, R. W.: Spurious diapycnal mixing associated with advection in az-coordinate ocean model, *Monthly Weather Review*, 128, 538–564, 2000.
- Ilicak, M., Adcroft, A. J., Griffies, S. M., and Hallberg, R. W.: Spurious dianeutral mixing and the role of momentum closure, *Ocean Modelling*, 45, 37–58, 2012.
- Jackett, D. R. and McDougall, T. J.: A neutral density variable for the world's oceans, *Journal of Physical Oceanography*, 27, 237–263, doi:10.1175/1520-0485(1997)027<0237:andvft>2.0.co;2, <GotoISI>://WOS:A1997WK25500002, 279, 1997.
- Klocker, A. and McDougall, T. J.: Influence of the Nonlinear Equation of State on Global Estimates of Dianeutral Advection and Diffusion, *Journal of Physical Oceanography*, 40, 1690–1709, doi:10.1175/2010jpo4303.1, <GotoISI>://WOS:000281520800002, klocker, Andreas/E-4632-2011 Klocker, Andreas/0000-0002-2038-7922 30, 2010.
- Klocker, A., McDougall, T., and Jackett, D.: A new method for forming approximately neutral surfaces, *Ocean Science*, 5, 155–172, 2009.
- Kuhlbrodt, T. and Gregory, J.: Ocean heat uptake and its consequences for the magnitude of sea level rise and climate change, *Geophysical Research Letters*, 39, 2012.
- Lee, M.-M., Coward, A. C., and Nurser, A. G.: Spurious diapycnal mixing of the deep waters in an eddy-permitting global ocean model, *Journal of Physical Oceanography*, 32, 1522–1535, 2002.
- Lumpkin, R. and Speer, K.: Global ocean meridional overturning, *Journal of Physical Oceanography*, 37, 2550–2562, 2007.
- McDougall, T. J.: NEUTRAL SURFACES, *Journal of Physical Oceanography*, 17, 1950–1964, doi:10.1175/1520-0485(1987)017<1950:ns>2.0.co;2, <GotoISI>://WOS:A1987L289100008, 220, 1987a.
- McDougall, T. J.: THERMOBARICITY, CABBELING, AND WATER-MASS CONVERSION, *Journal of Geophysical Research-Oceans*, 92, 5448–5464, doi:10.1029/JC092iC05p05448, <GotoISI>://WOS:A1987H434300036, 134, 1987b.
- McDougall, T. J. and Church, J. A.: Pitfalls with the Numerical Representation of Isopycnal Diapycnal Mixing, *Journal of Physical Oceanography*, 16, 196–199, 1986.
- McDougall, T. J. and Jackett, D. R.: On the helical nature of neutral trajectories in the ocean, *Progress in Oceanography*, 20, 153–183, doi:10.1016/0079-6611(88)90001-8, <GotoISI>://WOS:A1988T679900001, 26, 1988.
- McDougall, T. J. and Jackett, D. R.: An assessment of orthobaric density in the global ocean, *Journal of Physical Oceanography*, 35, 2054–2075, 2005.
- McDougall, T. J., Groeskamp, S., and Griffies, S. M.: On geometrical aspects of interior ocean mixing, *Journal of Physical Oceanography*, 44, 2164–2175, 2014.
- Megann, A.: Estimating the numerical diapycnal mixing in an eddy-permitting ocean model, *Ocean Modelling*, 121, 19 – 33, doi:https://doi.org/10.1016/j.ocemod.2017.11.001, http://www.sciencedirect.com/science/article/pii/S1463500317301762, 2018.
- Munk, W. and Wunsch, C.: Abyssal recipes II: energetics of tidal and wind mixing, *Deep-Sea Research Part I-Oceanographic Research Papers*, 45, 1977–2010, doi:10.1016/s0967-0637(98)00070-3, <GotoISI>://WOS:000077617000001, 837, 1998.

- Munk, W. H.: Abyssal recipes, in: *Deep Sea Research and Oceanographic Abstracts*, vol. 13, pp. 707–730, Elsevier, 1966.
- Nikurashin, M. and Vallis, G.: A Theory of Deep Stratification and Overturning Circulation in the Ocean, *Journal of Physical Oceanography*, 41, 485–502, doi:10.1175/2010jpo4529.1, <GotoISI>://WOS:000289325200007, nikurashin, Maxim/J-3506-2013 31, 2011.
- 5 Nikurashin, M. and Vallis, G.: A Theory of the Interhemispheric Meridional Overturning Circulation and Associated Stratification, *Journal of Physical Oceanography*, 42, 1652–1667, doi:10.1175/jpo-d-11-0189.1, <GotoISI>://WOS:000310183000003, nikurashin, Maxim/J-3506-2013 24, 2012.
- Redi, M. H.: Oceanic isopycnal mixing by coordinate rotation, *Journal of Physical Oceanography*, 12, 1154–1158, 1982.
- Saenz, J. A., Tailleux, R., Butler, E. D., Hughes, G. O., and Oliver, K. I. C.: Estimating Lorenz’s Reference State in an Ocean with a Nonlinear Equation of State for Seawater, *Journal of Physical Oceanography*, 45, 1242–1257, doi:10.1175/jpo-d-14-0105.1, <GotoISI>://WOS:000354370700003, 1, 2015.
- 10 Speer, K. G.: A note on average cross-isopycnal mixing in the North Atlantic ocean, *Deep-Sea Research Part I-Oceanographic Research Papers*, 44, 1981–1990, doi:10.1016/s0967-0637(97)00054-x, <GotoISI>://WOS:000072760700004, speer, KG, 1997.
- Tailleux, R.: Generalised Patched Potential Density and Thermodynamic Neutral Density: Two new physically-based quasi-neutral density variables for ocean water mass analyses and circulation studies, *Journal of Physical Oceanography*, 2016a.
- 15 Tailleux, R.: Neutrality Versus Materiality: A Thermodynamic Theory of Neutral Surfaces, *Fluids*, 1, 32, 2016b.
- Urakawa, L., Saenz, J., and Hogg, A.: Available potential energy gain from mixing due to the nonlinearity of the equation of state in a global ocean model, *Geophysical Research Letters*, 40, 2224–2228, 2013.
- Vallis, G. K.: Large-scale circulation and production of stratification: Effects of wind, geometry, and diffusion, *Journal of Physical Oceanography*, 30, 933–954, doi:10.1175/1520-0485(2000)030<0933:lscapo>2.0.co;2, <GotoISI>://WOS:000087152900010, 64, 2000.
- 20 Veronis, G.: The role of models in tracer studies, *Numerical models of ocean circulation*, pp. 133–146, 1975.
- Walin, G.: ON THE RELATION BETWEEN SEA-SURFACE HEAT-FLOW AND THERMAL CIRCULATION IN THE OCEAN, *Tellus*, 34, 187–195, <GotoISI>://WOS:A1982NJ88300010, 180, 1982.
- Winters, K. B. and D’Asaro, E. A.: Diascalar flux and the rate of fluid mixing, *Journal of Fluid Mechanics*, 317, 179–193, 1996.
- Winters, K. B., Lombard, P. N., Riley, J. J., and D’Asaro, E. A.: Available potential energy and mixing in density-stratified fluids, *Journal of Fluid Mechanics*, 289, 115–128, doi:10.1017/S002211209500125X, http://journals.cambridge.org/article_S002211209500125X, 1995.
- 25 Wolfe, C. L. and Cessi, P.: What Sets the Strength of the Middepth Stratification and Overturning Circulation in Eddy Ocean Models?, *Journal of Physical Oceanography*, 40, 1520–1538, doi:10.1175/2010jpo4393.1, <GotoISI>://WOS:000280899300006, 30, 2010.